Novel Preparation and Properties of Polypropylene−Vermiculite Nanocomposites

S. C. Tjong,*,† Y. Z. Meng,†,‡ and A. S. Hay§

Department of Physics & Materials Science, City University of Hong Kong, 83 Tat Chee Avenue, Kowloon, Hong Kong, Guangzhou Institute of Chemistry, Chinese Academy of Sciences, P.O. Box 1122, Guangzhou 510650, P. R. China, and Department of Chemistry, McGill University, 801 Sherbrooke Street West, Montreal, Quebec H3A 2K6, Canada

Received January 24, 2001. Revised Manuscript Received August 8, 2001

A novel approach to the preparation of polymer nanocomposites utilizing a low-molecular-weight reactive modifying reagent has been developed in this study. This is the first report on the fabrication of in situ nanocomposites using maleic anhydride as a reactive reagent that acts both as a modifying additive for the polymeric matrix and as a swelling agent for the silicate. Accordingly, polypropylene−vermiculite nanocomposites with an intercalated or exfoliated structure can be achieved by simple melt mixing of maleic anhydride-modified vermiculite with polypropylene. The nanocomposite structure is evidenced by the absence of vermiculite reflections in the X-ray powder diffraction patterns. Tensile tests show that the tensile modulus and strength of the nanocomposites tend to increase dramatically with vermiculite addition. Such enhancement in mechanical properties results from the formation of intercalated and exfoliated vermiculite reinforcement in the composites. Finally, the thermal properties of the nanocomposites were investigated by means of dynamic mechanical analysis (DMA), differential scanning calorimetry (DSC), and thermogravimetric analysis (TGA). The effects of maleic anhydride addition on the formation of nanometric reinforcement and on the mechanical properties of nanocomposites are discussed.

Introduction

In conventional filled polymer composites, the fillers are dispersed nonuniformly in the polymer matrix, thereby producing phase-separated macrocomposites. The applied load is transferred to the filler via the matrix−filler interfaces. Inorganic fillers are known to have little interaction with organic polymers, leading to poor bonding with the matrix. The filler content normally must exceed 30% to achieve an optimum reinforcement for thermoplastics. The addition of inorganic fillers to thermoplastics also results in a dramatic increase in the processing melt viscosity of the composites.

Since the first report of organoclay hybrid polyamide nanocomposites by Fujiwara and Sakomoto[1] of the Unichika Co. in 1976, polymer-layered silicate nanocomposites have attracted considerable attention from polymer scientists. In such novel materials, molecular or nanoscale reinforcements rather than conventional particulates or fibers are used.[2,3] Consequently, nanocomposites exhibit markedly improved mechanical properties because of the nanometer-scale dispersion of reinforcements and the high surface-to-volume ratio.[4] Clays are commonly used as additives for polymers because they are composed of layered silicates that can intercalate with organic molecules. Silicates, such as montmorillonite, hetorite, and mosco-clay, have been used as reinforcing fillers for polymers because of their potentially high aspect ratios.[5−9] They exhibit a layered structure (around 1 nm in thickness) and form platelets of approximately 30−50 nm in the lateral dimensions, if properly exfoliated.[9] These platelets exhibit very high stiffness and strength when dispersed uniformly in the polymer matrix. From these aspects, the advantages of developing nanocomposite technology using clay minerals include (a) low loading levels of silicates, (b) transparency and incorporation of flexibility in the formed nanocomposites, (c) synergies with other additives, and (d) low cost.

To achieve a nanoscale dispersion of silicates in a polymer matrix, the silicates are generally pretreated with alkylammonium ions or reactive organic compounds to produce an organoclay.[10] This treatment improves the affinity between the hydrophilic silicate

* Corresponding author: S. C. Tjong. Tel.: +852-27887702. Fax: +852-27887830. E-mail: aptjong@cityu.edu.hk.
† City University of Hong Kong.
‡ Chinese Academy of Sciences.
§ McGill University.

(1) Fujiwara S.; Sakamoto, T. Japanese Patent No. 109998, **1976**.
(2) Burnside, S. D.; Glannelis, E. P. *Chem. Mater.* **1995**, *7*, 1597.
(3) Giannelis, E. P. *Appl. Organomet. Chem.* **1998**, *12*, 675.
(4) Gonsalves, K.; Chen, X. *Mater. Res. Soc. Symp. Proc.* **1996**, *435*, 55.
(5) Vaia, R. A.; Jandt, K. D.; Kramer, E. J.; Giannelis, E. P. *Macromolecules* **1995**, *28*, 8080.
(6) Akelah, A.; Salahuddin, N.; Hiltner, A.; Baer, E.; Moet, A. *Nanostruct Mater.* **1994**, *4*, 965.
(7) Pinnavaia, T. J. *Science* **1983**, *220*, 365.
(8) Mehrotra, V.; Giannelis, E. P. *Mater. Res. Soc. Symp. Proc.* **1990**, *171*, 39.
(9) Alexandre, M.; Dubois, P. *Mater. Sci. Eng., R.* **2000**, *28*, 1.
(10) Giannelis, E. P. *Adv. Mater.* **1996**, *8*, 29.

10.1021/cm010061b CCC: $22.00
Published on Web 12/20/2001

and hydrophobic polymer. The organoclays can then be easily dispersed in the polymer matrix and form nanocomposites with an intercalated or exfoliated structure. In the former case, the spacing between the silicate layers is increased by the incorporation of extended polymer chains into the layers. In exfoliated nanocomposites, unstacked organoclay blocks are dispersed individually throughout the polymer matrix.[11] In general, melt compounding of polar polymer matrixes with organoclays can lead to nanocomposites with exfoliated structures, e.g., exfoliated poly(dimethylsiloxane),[2] epoxy,[12] nylon-6,[13−14] polycaprolactone,[15] and polyacrylonotrile[16] nanocomposites. However, intercalated structures can only be prepared from polymers with nonpolar chains, such as polyolefins,[10] polystyrene,[17] and poly(ethylene oxide).[18] More recently, Vaia et al. suggested that polymer−clay nanocomposites can be fabricated via direct polymer melt intercalation in which the polymer chains are diffused into the space between the silicate layers or galleries.[5,19−20] Conventional polymer processing techniques such as extrusion can reduce the time for nanocomposites fabrication through its ability to break up the silicate layers. Apparently, this is a newer approach to the preparation of nanocomposites with promising commercial applications. However, little information is available in the literature on the fabrication of nanocomposites via direct melt blending.[21−24] The mechanisms responsible for nanostructure formation remain unclear. It is generally believed, at least, that several key parameters can affect the dispersion of the organoclay in the polymeric matrix via melt compounding, e.g., mixing rate, time, and temperature.

In this paper, we attempt to develop a new processing route to the in situ preparation of nanocomposites based on polyolefin and silicate. This approach allows for the intercalation or exfoliation of silicate layers via in situ or direct melt compounding of silicate clay and polypropylene in a Brabender extruder. The morphology and thermal and mechanical properties of the resulting nanocomposites are studied.

Experimental Section

Materials. The vermiculite used in this work was purchased from Aldrich with grade number 3. Its physical and chemical properties are listed in Table 1. PP polymer (Profax 6331) with a melt flow index of 12 g/10 min was purchased from Himont Company. The maleic anhydride (MA) supplied by Fluka Chemie and dicumyl peroxide (DCP) produced by Aldrich chemical company were used as received. Other reagent-grade chemicals were also used.

Table 1. Composition and Properties of Vermiculite

particle size (mesh)	surface area (m^2/g)	content (%)						
		SiO_2	Al_2O_3	MgO	Fe_2O_3	CaO	K_2O	C
<10	<1	45	9	21.5	6	5	1	0.2

Organo-Vermiculite Preparation. The vermiculite was first pretreated with hydrochloric acid according to a reported patent.[25] Approximately 25 g of the crude vermiculite was introduced into 1 L of a 2 M HCl solution in a polypropylene beaker at room temperature. The resulting slurry was magnetically stirred for 8 h. The pH of the slurry was adjusted to 3.0−4.0. The vermiculite was then separated by filtering and washed thoroughly with distilled water several times until the filtrate had a pH value of 7.0. Following washing, the obtained solid material was dried at 160 °C overnight. The final product after grinding was a fine powder with as-received color. The delamination process of vermiculite was controlled and monitored by X-ray diffraction. The acid-delaminated vermiculite was then further treated with MA. To a 250-mL PP beaker were charged 50 g of MA, 50 g of acid-treated vermiculite, and 100 mL of acetic acid. The slurry was magnetically stirred for 12 h. The resulting slurry was dried in a rotary evaporator at 60 °C and subsequently dried in an oven at 70 °C for 24 h under vacuum. The final MA-pretreated vermiculite in the form of fine powder was kept in a dryer.

Nanocomposite Preparation. MA-pretreated vermiculite (MAV) was prepared in a twin-screw Brabender Plasticorder at 15−35 rpm by a one-step reaction of PP with MAV in the presence of DCP. The compounding temperature profiles selected were 200−220−230−180 °C. The weight ratios of PP to MAV to DCP were fixed at 96:4:0.3 and 90:10:0.3. The nanocomposites with the latter ratio were melt blended at speeds of 15 and 35 rpm. The extrudates were then pelletized after exiting from the extruder. These nanocomposites are designated as PP(MAV)-*x*/*y* throughout this paper, where *x* is the weight percent of vermiculite and *y* is the screw speed of the Brabender. For example, the nanocomposite with the weight ratio of PP to MAV to DCP maintained at 96:4:0.3 and compounded at 15 rpm is designated PP(MAV)-2/15.

The PP(MAV) nanocomposite pellets were dried in an oven for 8 h at 100 °C prior to injection molding. Subsequently, the PP(MAV) pellets were injection molded into standard dog-bone tensile bars (ASTM D638). The mold temperature was maintained at 40 °C, and the barrel zone temperatures were set at 210, 220, and 220 °C. An injection pressure of 70 bar and a holding pressure of 40 bar were used.

Mechanical Measurements. The tensile behavior of the nanocomposites was determined using an Instron tensile tester (model 4206) at 23 °C. A cross-head speed of 5 mm min^{-1} was used in the measurements. Dynamic mechanical analysis (DMA) of the injection molded composites was conducted with a Du Pont DMA (model 983) at a fixed frequency of 1 Hz and an oscillation amplitude of 0.2 mm. The temperatures studied ranged from −30 to 170 °C, with a heating rate of 2 °C min^{-1}.

Morphological Observations. The injection-molded bars were fractured in liquid nitrogen. The morphologies of the specimens were observed by transmission electron microscope (TEM, Philips CM20) and scanning electron microscope (SEM, JEOL JSM model 820). For the TEM examinations, ultrathin specimens with a thickness of about 50 nm were cut from the middle section of the injection-molded bars parallel to the flow direction. Cutting operations were carried out using a Reichert Ultracut S microtome under cryogenic conditions, and the film was retrieved onto Cu grids. The thin films (∼5 nm) were stained for 5 h in OsO_4 solution and then coated with a very thin layer of carbon prior to TEM examination.

Thermal Analyses. The decomposition of the composites from 30 to 600 °C was determined with a Seiko thermogravimetric analyzer (TGA, model SSC-5200) under a protective helium atmosphere (200 mL/min). The heating rate employed was 10 °C min^{-1}. The glass transition temperatures (T_g) were

(11) Carrado, K.; Xu, L. *Chem. Mater.* **1998**, *10*, 1440.
(12) Messersmith, P. B.; Giannelis, E. P. *Chem. Mater.* **1993**, *5*, 1064.
(13) Fukushima, Y.; Okada, A.; Kawasumi, M.; Kurauchi, T.; Kamigaito, O. *Clay Miner.* **1988**, *23*, 27.
(14) Cho, J. W.; Paul, D. R. *Polymer* **2001**, *42*, 1083.
(15) Novak, B. M. *Adv. Mater.* **1993**, *5*, 422.
(16) Vaia, R. A.; Sauer, B. B.; Tse, O. K.; Giannelis, E. P. *J. Polym. Sci. B: Polym. Phys.* **1997**, *35*, 59.
(17) Wang, M. S.; Pinnavaia, T. J. *Chem. Mater.* **1994**, *6*, 468.
(18) Akelah, A.; Moet, A. J. *Mater. Sci.* **1996**, *31*, 3589.
(19) Vaia, R. A.; Giannelis, E. P. *Macromolecules* **1997**, *30*, 7990.
(20) Vaia, R. A.; Giannelis, E. P. *Macromolecules* **1997**, *30*, 8000.
(21) Maxfield, M.; Christiani, B. R.; Murthy, S. N.; Tuller, H. U.S. Patent 5,385,776, 1995.
(22) Christiani, B. R.; Maxfield, M. U.S. Patent 5,7475,60, 1998.
(23) Kawasumi, M.; Hasegawa, N.; Kato, M.; Usuki, A. *Macromolecules* **1997**, *30*, 6333.
(24) Liu, L.; Qi, Z.; Zhu, X. *J. Appl. Polym. Sci.* **1999**, *71*, 1133.
(25) Rittler, H. R. U.S. Patent 4,952,388, 1990.

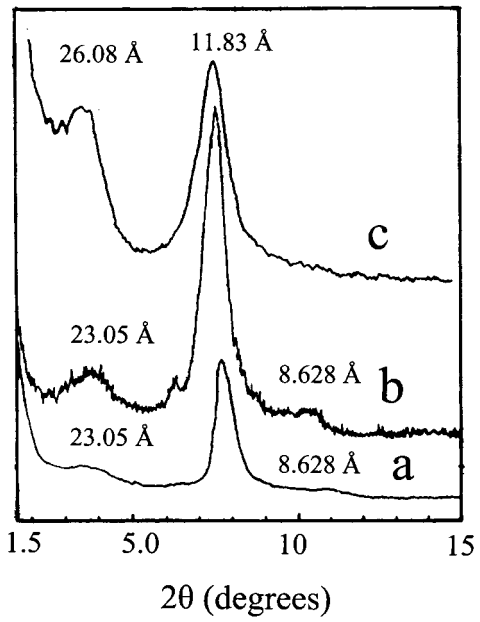

Figure 1. X-ray diffraction patterns of vermiculite (a) as-received without any treatment, (b) upon heating for 24 h at 160 °C, and (c) acid-delaminated using 2 M HCl followed by drying at 160 °C overnight.

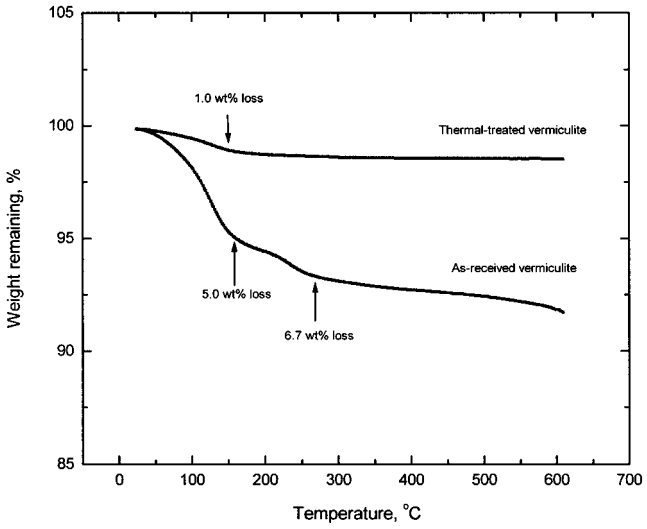

Figure 2. Thermogravimetric curves for as-received and thermally treated vermiculites.

determined with Perkin-Elmer 7C DSC instrument at a heating rate of 20 °C min^{-1} under nitrogen flow.

X-ray Diffraction Analyses. X-ray diffraction (XRD) patterns were obtained with a Rigaku RINT X-ray diffractometer (model DMAX 1200) using Ni-filtered Cu Kα radiation. Samples of varying vermiculite contents were ground into powders, and the patterns were recorded in the reflection mode for $2\theta = 1.5-15°$, using a scanning speed and step size of 2° and 0.05°, respectively. In the case of the nanocomposites, measurements were carried out on the powders of the specimens.

Results and Discussion

Delamination of Vermiculite. Vermiculite is a clay mineral consisting of silicate layers with a thickness of about 1 nm. Such layers are composed of octahedral alumina or magnesia sandwiched between two tetrahedral silicate sheets. When trivalent aluminum ions are partially substituted by divalent magnesium ions,

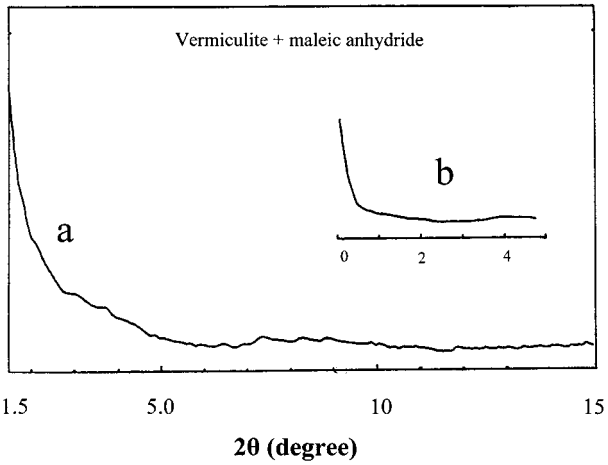

Figure 3. X-ray diffraction patterns of MAV recorded by (a) wide angle ranging from 1.5 to 15° and (b) small angle ranging from 0 to 5°.

Table 2. Interlayer Platelet Spacings of Vermiculite after Different Treatments

vermiculite	spacing (Å), content (%)	spacing (Å), content (%)	spacing (Å), content (%)	spacing (Å), content (%)
as-received	no	23.05 (6.4)	11.83 (92)	8.628 (1.6)
thermally treated	no	23.05 (9.6)	11.83 (89.4)	8.628 (1.0)
HCl-treated	26.08 (41.8)	no	11.83 (58.2)	no
MA-treated	no	no	no	no

the individual layers are negatively charged. Electroneutrality is maintained by alkali cations such as sodium or potassium located in the interlayer galleries.[19] Various methods have been proposed for the delamination of vermiculite. For example, vermiculite can be pretreated by a surfactant to produce an organoclay,[10,26] by the ion-exchange method,[27,28] or by direct heating in a reactive vapor phase.[29]

In this work, we have used the acid-treatment route to delaminate the vermiculite. Figure 1 shows the X-ray diffraction patterns of vermiculite after different treatments. As-received vermiculite yields characteristic diffraction peaks at $2\theta = 3.833$, 7.484, and 10.286° (Figure 1a). From XRD measurements, the interlayer platelet spacings (001 diffraction peak) and their contents were determined. The results are summarized in Table 2. The basal plain portion with a spacing of 11.83 Å is the dominant product, as indicated in the table. Such a spacing is different from that of sodium montmorillonite, which has a spacing of 0.96 nm.[30] Moreover, it also contains a 6.4% fraction with an expanded spacing of 23.05 Å. The vermiculite dried at 160 °C for 24 h (Figure 1b) has 9.6% of a fraction with a spacing of 23.05 Å, demonstrating that hydrated silicate can be dehydrated and delaminated by proper thermal treatment. The thermogravimetric (TG) curves (Figure 2) indicate that the original vermiculite contains about 2% water, which can be removed by simply drying. For the HCl-treated vermiculite, the diffraction peak with a

(26) Burnside, S. D.; Wang, H. C. *Chem. Mater.* **1999**, *11*, 1055.
(27) Osman, M. A.; Caseri, W. R.; Suter, U. W. *J. Colloid Interface Sci.* **1998**, *198*, 157.
(28) Rittler, H. R. U.S. Patent 4,715,987, 1987.
(29) Rittler, H. R. U.S. Patent 4,826,628, **1989**.
(30) Fu, X.; Qutubuddin, S. *Polymer* **2001**, *42*, 807.

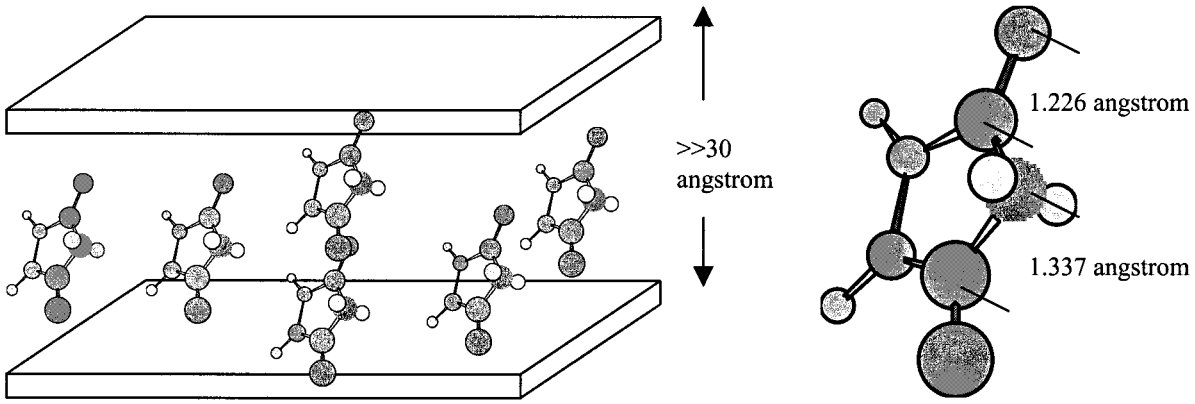

Figure 4. Structures for energy-minimized maleic anhydride and MAV.

spacing of 23.05 Å is broadened and partially shifted to $d = 26.08$ Å. This is 3.03 Å higher than the peak position for the as-received vermiculite (Figure 1c). The delaminated content is further increased up to 41.8%. It should be noted that the delamination of vermiculite must be controlled within a specific period of time because prolonged treatment can cause destruction of the unit cell structure through excessive cleavage or scission of the bonds other than the cation−hydroxyl bonds. We conclude that the optimum time is ~8 h.

To further delaminate the vermiculite layers, partially delaminated vermiculite was exposed to a mixed MA and acetic acid solution and stirred for 12 h. Both WXRD and SXRD diffraction traces of MAV (Figure 3) indicate the absence of diffraction peaks, which clearly reveals that the vermiculite is further delaminated, according to the literature.[31] MA can easily enter the galleries of acid-treated vermiculite because solvent (acetic acid) can act as a carrier to transport MA into hydrophilic vermiculite. MA has a flat molecular structure in which the greatest length is about 5.126 Å, as depicted in Figure 4. This figure also reveals that the incorporation of excess MA into acid-treated vermiculite extends its gallery spacing.

Exfoliation of Maleic Anhydride Delaminated Vermiculite by in Situ Melt Compounding. In previous studies, MA-compatibilized polypropylene (MPP) hybrid macrocomposites reinforced with various fiber reinforcements, such as whiskers, liquid-crystalline polymers, and glass fibers, were prepared in a twin-screw extruder.[32−35] It is well-documented that MA can be readily melt grafted onto PP chains, thereby improving the affinity between the resulting MPP and various inorganic reinforcements. In this respect, it is considered that PP can be melt blended with MAV that is completely delaminated by MA to form a ternary molecular structure of vermiculite/MA/PP in the presence of DCP. In such a compatiblized structure, grafted MA acts as a center or bridge to bond the vermiculite and PP together. A model of this structure is depicted in Figure 5. It is worth noting that the in situ reaction between MAV and PP and the associated shear forces within the extruder are the driving force for further delamination

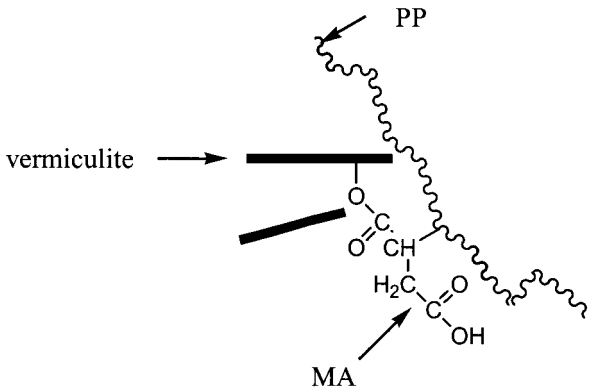

Figure 5. Ternary vermiculite/MA/PP molecular structure.

Table 3. Processing Conditions Used in This Study

equipment type	processing conditions
twin-screw extruder (Brabender Plasticorder)	temperature profile 200−220−220−180 °C, screw speed 15−35 rpm
injection molder	temperature profile 170−180−180 °C, injection pressure 50 bar, holding pressure 40 bar, molding temperature 40 °C

or exfoliation of MAV. Moreover, evaporation of MA could also intercalate or exfoliate vermiculite because MA can be easily evaporated during melt compounding of PP. The processing conditions used in this work are listed in Table 3. Figure 6 shows the X-ray diffraction patterns of the extruded nanocomposites PP(MAV)-2/15, PP(MAV)-5/15, and PP(MAV)-5/35. Apparently, there are no characteristic peaks from 1.5 to 10°, indicating that all three nanocomposites are completely intercalated or exfoliated despite the different screw speeds and vermiculite loadings employed. These results are consistent with the above-described exfoliation mechanism, i.e., the driving forces for vermiculite exfoliation result from MA evaporation and its grafting onto molten PP.

Mechanical Properties. The mechanical properties of PP/MAV nanocomposites are summarized in Table 4. It can be seen that the tensile strengths of the nanocomposites increase dramatically with increasing MAV contents. The tensile strength of PP is increased by 18.3% with the addition of only 2% vermiculite and by up to 29.5% when 5% vermiculite is introduced. This beneficial effect is believed to arise from an improvement of the compatibility between the vermiculite and PP matrix associated with MA addition. In other words, grafting reactions between MA, vermiculite, and PP are responsible for the compatibilizing effect of MA on PP/

(31) Kornmann, X.; Lindberg, H.; Berglund, L. A. *Polymer* **2001**, *42*, 1303.
(32) Tjong, S. C.; Meng, Y. Z. *Polymer* **1997**, *38*, 4609.
(33) Tjong, S. C.; Meng, Y. Z. *Polymer* **1998**, *39*, 54 61.
(34) Meng, Y. Z.; Tjong, S. C. *Polymer* **1998**, *39*, 99.
(35) Tjong, S. C.; Meng, Y. Z. *Polymer* **1999**, *40*, 7275.

Table 4. Mechanical Properties of PP/Vermiculite Nanocomposites

nanocomposite	vermiculite content (%)	tensile strength (MPa)	tensile modulus (MPa)	storage modulus[a] (GPa)	elongation at break (%)	energy at break (J)
PP	0	28.80	843.6	0.78	670.0	229.2
MPP	0	27.90	725.1	0.76	697.0	202.7
PP(MAV)-2/15	2	34.08	1010.0	2.37	18.89	13.04
PP(MAV)-5/15	5	35.28	1197.0	2.77	10.37	12.78
PP(MAV)-5/35	5	37.30	1297.0	3.32	10.23	12.87

[a] Obtained from DMA analyses at 25 °C.

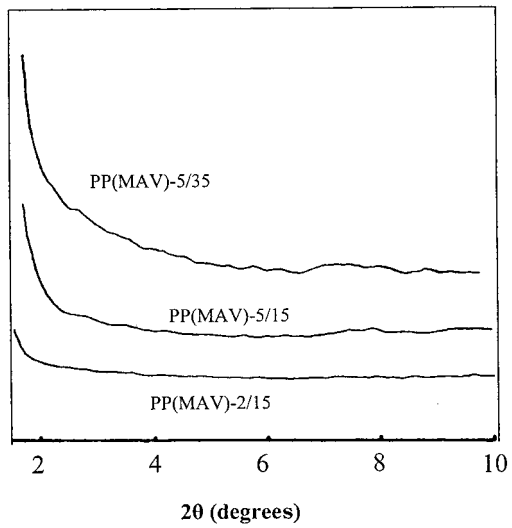

Figure 6. X-ray powder patterns for nanocomposites PP(MAV)-2/15, PP(MAV)-5/15, and PP(MAV)-5/35 formed in the twin-screw extruder.

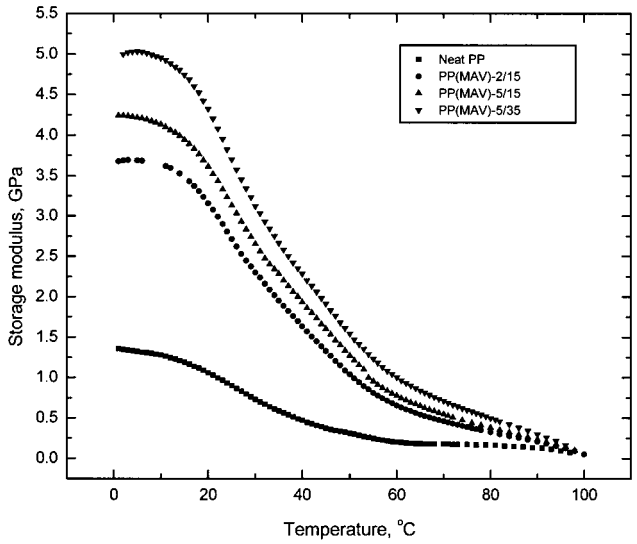

Figure 7. Storage modulus versus temperature for neat PP and PP(MAV) nanocomposites.

MAV nanocomposites. Consequently, a ternary molecular structure of vermiculite/MA/PP with MA in the grafted PP as a center can develop in these nanocomposites (Figure 5). Moreover, the ternary structure can promote the dispersion of vermiculite within PP matrix. It is also noted that the tensile moduli, particularly the storage modulus (Table 4 and Figure 7), increase significantly upon formation of the nanocomposites. The moduli of the nanocomposites approach the maximum theoretical value expected from the theory of elasticity[36] because they are free from internal defects. The introduction of vermiculite into the PP matrix increases the stiffness at the expense of the toughness of the composites. Significant reductions in the elongation and energy at break are observed. The elongation and energy at break decrease sharply with MAV addition. This behavior is a typical characteristic of discontinuous fiber-reinforced polymer composites and similar to that observed in conventional composites reinforced with short glass fibers or whiskers.[33,34,37,38] It is noteworthy that an increase in compounding speed results in further improvement in the mechanical stiffness and strength (Table 4) because of thedue higher shear force applied to the vermiculite layers. As a result, the increased compounding speed enhances the dispersion of vermiculite in melt PP and the reinforcing efficiency of vermiculite on PP.

To assess the reinforcing efficiency, the mechanical properties of MPP composites with different reinforcements are listed in Table 5. It is apparent from this table that the stiffness and strength of PP/MAV nanocomposite are considerably higher than those of conventional macrocomposites containing the same reinforcement content such as MPP/$K_2Ti_6O_{13}$ and MPP/LCP macrocomposites.[39,40] In these conventional composites, the interfacial bonding between the matrix and the reinforcing materials is relatively poor. Thus, maleic anhydride is used to improve the interfacial adhesion between them. On the other hand, the maleic anhydride functional group of PP/MAV nanocomposites tends to intercalate and exfoliate the galleries of vermiculite, leading to nanoscale dispersion of reinforcement within the polymer matrix. Although the modulus of the MPP/$K_2Ti_6O_{13}$ composite is smaller than that of the PP/MAV nanocomposite, the former composite maintains a significant amount of ductility. The poor ductility of the PP/MAV nanocomposite presumably arises from excessive grafting reaction between the PP matrix and MA.

Morphology. Figure 8a,b shows TEM images of the PP(MAV)-5/15 nanocomposite. TEM samples were prepared from the injection-molded tensile bars. The vermiculite was oriented and intercalated or exfoliated into fine layers that are parallel to the melt flow direction, as shown in Figure 8a. A higher-magnification TEM image of the nanocomposite is presented in Figure 8b, where individual vermiculite layers appear as dark gray lines. Moreover, some clusters or stacks of vermiculite are observed as thick dark lines along the melt flow direction (Figure 8a). These clusters or stacks exhibit a ribbonlike fibrillar morphology in the PP(MAV)-5/15 nanocomposite. For the PP(MAV)-5/35 nano-

(36) Coutnet T. H. *Mechanical Behavior of Materials*; McGraw-Hill: New York, 1990; pp 83−84.
(37) Datta, A.; Baird, D. G. *Polymer* **1995**, *36*, 505.
(38) O'Donnell, H. J.; Baird, D. G. *Polymer* **1995**, *36*, 3113.
(39) Tjong, S. C.; Meng, Y. Z. *J. Appl. Polym. Sci.* **1998**, *70*, 431.
(40) Meng, Y. Z.; Tjong, S. C. *Polym. Compos.* **1998**, *19*, 1.

Table 5. Mechanical Properties of PP Composites with Different Reinforcements

composite	reinforcement content (%)	tensile strength (MPa)	tensile modulus (MPa)	storage modulus[a] (GPa)	elongation at break (%)
PP	0	28.80	843.6	0.78	670.0
MPP	0	27.90	725.1	0.76	697.0
PP(MAV)-5/35	5	37.30	1297.0	3.32	10.23
MPP/$K_2Ti_6O_{13}$[39]	5	31.80	1076.0	3.12	432.0
MPP/LCP[40]	5	31.50	864.3	2.72	92.00

[a] Obtained from DMA analyses at 25 °C.

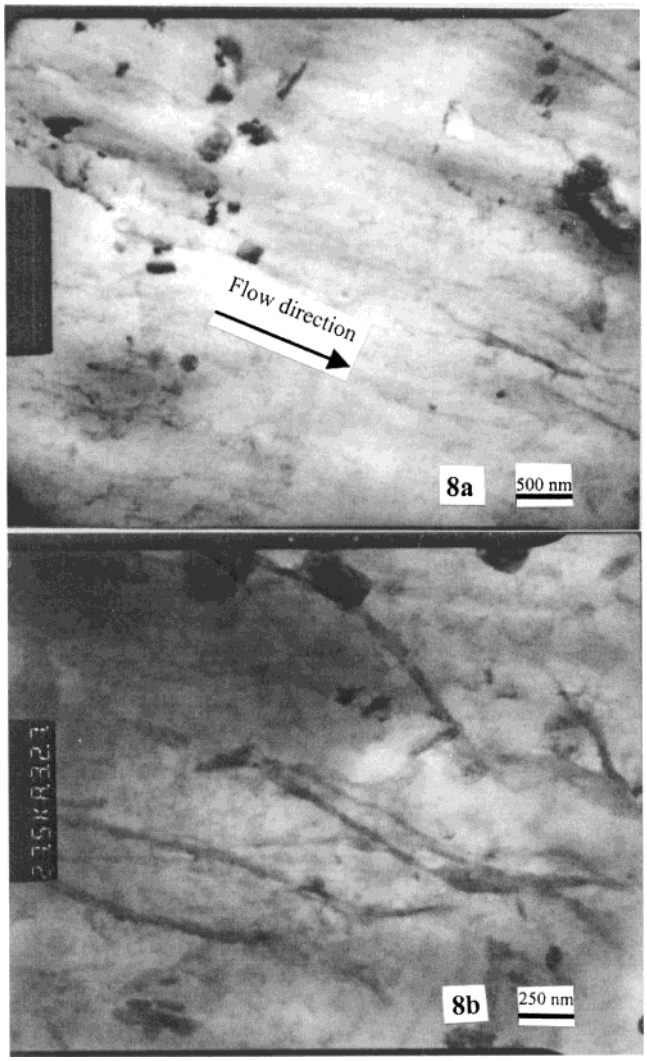

Figure 8. Typical TEM micrographs of PP(MAV)-5/15 nanocomposite showing (a) formation of exfoliated vermiculite layers in the composite and (b) enlarged image of exfoliated vermiculite layers.

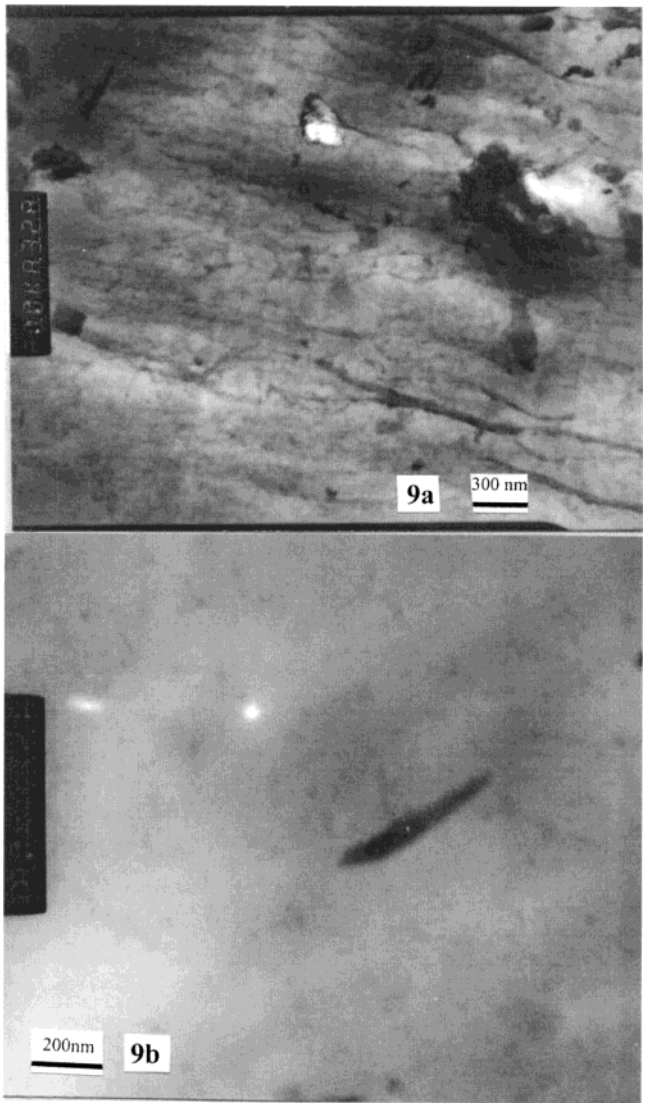

Figure 9. Typical TEM micrographs of PP(MAV)-5/35 nanocomposite showing (a) formation of exfoliated vermiculite layers in the composite and (b) enlarged image of exfoliated vermiculite layers.

composite prepared at a screw speed of 35 rpm, the TEM micrographs show a similar morphology of vermiculite within the PP matrix (Figure 9a,b). From a comparison of Figures 8b and 9a, it can be seen that an increase in the compounding speed or shear rate leads to a higher degree of intercalation or exfoliation of vermiculite in melt PP. From Figure 9b, the vermiculite layer cell exhibits a thickness of ∼2 nm and a length of 200 nm, indicating that the vermiculite layers have a very large aspect ratio.

Figure 10a,b shows the SEM micrographs of nanocomposite PP(MAV)-5/35. Individual vermiculite layers can be readily seen in the SEM micrograph (Figure 10a). A higher-magnification view of the sample reveals that good adhesion exists between the vermiculite layers and the PP matrix as a result of the presence of MA (Figure 10b). It should be noted that both the average thickness and the length deduced from the SEM photomicrographs are somewhat higher than those observed from the corresponding TEM micrographs. The resolution of electron microscopes depends on the electron wavelength and aberration of the lenses. TEM generally exhibits a much higher image resolution than SEM because the magnetic lenses of TEM have lower spherical aberrations. Moreover, TEM is operated at higher voltages, e.g., 100−200 kV compared to SEM at 20−30 kV. This implies that the wavelength of electrons is shorter in TEM than in SEM.[41] Other possible explana-

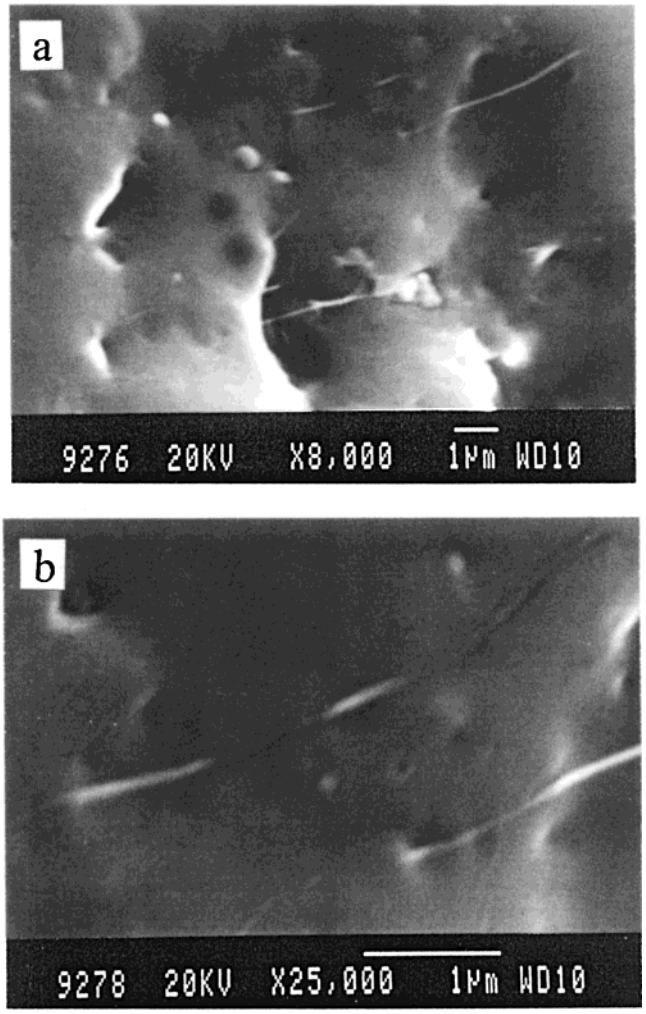

Figure 10. SEM micrographs of PP(MAV)-5/35 nanocomposite showing (a) formation of exfoliated vermiculite layers in the composite and (b) enlarged image of exfoliated vermiculite layers.

Table 6. Thermal Properties of PP/MAV Nanocomposites

specimen	T_g[a] (°C)	T_{new} (°C)	T_m[b] (°C)	$T_{-5\%}$[c] (°C)	T_{max}[c] (°C)
PP	15.80	–	171.1	309.5	428.3
PP(MAV)-2/15	15.89	66.17	172.0	290.6	444.5
PP(MAV)-5/15	18.85	66.99	170.9	282.7	449.1
PP(MAV)-5/35	17.58	67.06	170.5	278.0	449.9

[a] T_g values determined by DMA. [b] T_m values determined by DSC. [c] $T_{-5\%}$ and T_{max} values determined by TGA.

tions are that the microtoming direction is not exactly perpendicular to the surface of the platelets and that the inhomogeneity in and between samples might lead to the differences between SEM and TEM images. Therefore, the image of the platelets appears to be thicker than the actual size.[14]

Thermal Properties. The thermal properties of pure PP and PP/MAV nanocomposites determined by DSC, DMA, and TGA are summarized in Table 6. It can be seen that the introduction of vermiculite results in a slight increase in the T_g of the PP matrix to 15.8 °C. Cho and Paul[14] reported that the presence of nanoscale filler does not affect the T_g of the PA6 matrix, but the crystalline melting points (T_m) of the nanocomposites

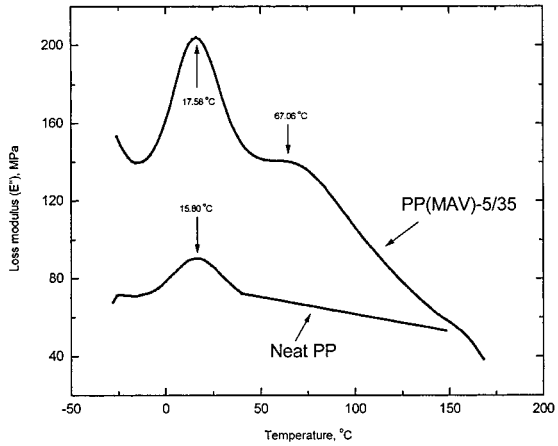

Figure 11. Loss modulus versus temperature for PP and PP-(MAV)-5/35 nanocomposite.

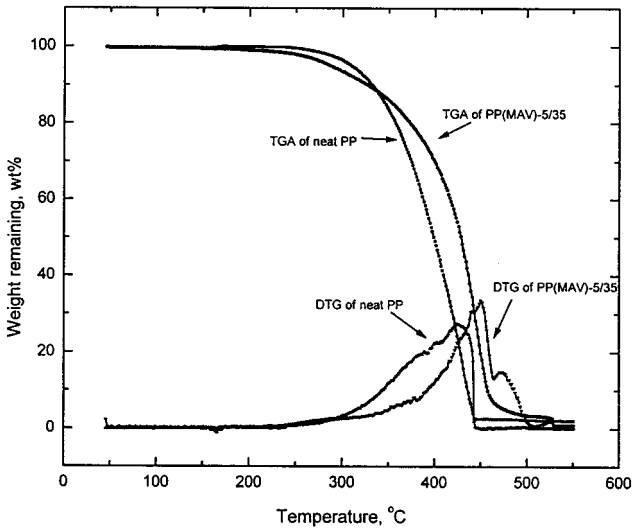

Figure 12. TG and DTG curves for neat PP and PP(MAV)-5/35 nanocomposites.

occur at temperatures slightly lower than the T_m of neat nylon 6. For PP/MAV nanocomposites, the mobility of PP molecular chains is restricted by the presence of vermiculite layers, leading to a slight increase in the T_g of the nanocomposites. However, the T_m of the nanocomposites shows little change because the nanoscale fillers do not alter the crystallite size.

Figure 11 shows the loss modulus versus temperature for PP and PP(MAV)-5/35 nanocomposite. A new peak appears at about 67 °C for the nanocomposite compared with neat PP. This behavior implies that a new microphase consisting of ternary molecule PP/MA/vermiculite is formed in the nanocomposite. Therefore, it is believed that the introduction of vermiculite does not change the crystalline morphology of the PP matrix, probably because of the relatively low loading and nanoscale size of vermiculite.

The TG curves of PP/MAV nanocomposites are shown in Figure 12. Both the 5% loss temperatures ($T_{-5\%}$) and the maximum weight loss temperatures (T_{max}) are listed in Table 6. This table reveals that the addition of MAV leads to a marked decrease in $T_{-5\%}$ from 309.5 to ~280 °C. This could arise because the acid-pretreated vermiculite contains excess MA. Unreacted MA could be easily sublimed, resulting in the decrease of $T_{-5\%}$

(41) Edington, J. W. *The Operation and Calibration of the Electron Microscopy*; Macmillan Press: London, 1974; pp 2−4.

because of the low melting temperature of MA. On the other hand, the T_{max} of the nanocomposites tends to increase considerably with the incorporation of vermiculite, clearly indicating that vermiculite exhibits a beneficial effect on the thermal stability of PP.

Conclusions

A novel approach to in situ polymeric nanocomposite preparation utilizing a low-molecular-weight reactive reagent is presented. The reactive reagent used is maleic anhydride, which acts both as a modifying additive for the polymeric matrix and as a swelling agent for the silicate. Accordingly, vermiculite/PP nanocomposites can be prepared by simple melt mixing of MAV and PP. The nanocomposite structure is evidenced by the absence of vermiculite reflections in the X-ray diffraction patterns. Moreover, SEM and TEM examinations provided more direct evidence for the formation of intercalated and exfoliated nanocomposites. The tensile moduli and strengths of the nanocomposites tend to increase dramatically with the addition of small amounts of vermiculite. Such an enhancement in mechanical properties results from the nanometric scale reinforcement of vermiculite in PP. TGA results showed that vermiculite improves the thermal stability of PP considerably. DMA profiles demonstrate that the nanocomposites exhibit the formation of a new microphase consisting of ternary PP/MA/vermiculite.

CM010061B